A Numerical Study addressing the Stress Distribution in Circular Steel Tube Confined Concrete Columns considering Various Concrete Strengths

Hoang An Le

Ho Chi Minh City University of Transport, Vietnam

hoangan.le@ut.edu.vn

(corresponding author)

ABSTRACT

The axially compressive behavior of Steel Tube Confined Concrete (STCC) columns has been experimentally investigated by many researchers throughout the world. However, it is extremely complicated to measure the stresses of steel tubes and concrete core in real tests. Therefore, to investigate the fundamental behavior of STCC columns under axial compression, this paper presents a numerical study that explores the stress distribution in steel tubes and concrete core. The circular STCC columns with the use of Normal Strength Concrete (NSC), High Strength Concrete (HSC), and Ultra-High Strength Concrete (UHSC) were simulated in a Finite Element Model (FEM) in ABAQUS. The material model for confined concrete incorporating a wide range of concrete strength values was developed in the simulation. The obtained from FEM curves of load versus strain of circular STCC columns were compared with those measured in real tests to verify the accurateness of the FEM. Deriving from the results of FEM, the stress states and their distribution in outer steel tubes and concrete core along the column height were described. Also, the longitudinal stresses on the cross-section of the concrete core were calculated corresponding with the load stage to quantify the strength enhancement of the concrete core due to the confinement effect from the steel tube. Furthermore, the confining pressure provided by the outer steel tube and impacting on the concrete core was plotted. Based on the findings in this paper, the effect of various concrete strengths on the stress distribution in circular STCC columns was investigated.

Keywords-steel tube confined concrete; NSC; HSC; UHSC; ABAQUS; FEM

I.   INTRODUCTION

It is widely known that the confinement effect in Concrete Filled Steel Tube (CFST) columns can result in remarkable improvements in compressive strength and ductility [1-11]. Therefore, CFST columns have been extensively applied in civil engineering projects. For this column type, when the steel tube and the concrete core are loaded simultaneously, the confining stress induced by the steel tube is less effective as compared to the case where only the concrete core is loaded [5-11]. If the ductility and strength of composite columns are considered as critical design factors, it is suggested that the load should be applied on the concrete core only in order to form Steel Tube Confined Concrete (STCC) columns [9]. Many previous studies have conducted experimental tests on the axial compressive behavior of STCC columns [1-4], but they have mainly focused on the use of Normal Strength Concrete (NSC) or High Strength Concrete (HSC). Recently, several studies have reported the test results of circular STCC columns infilled with Ultra-High Strength Concrete (UHSC) under axial compression [5, 10, 11, 19]. According to them, the

confining stress level in STCC columns depends on concrete strength. The dilation of concrete under compression is higher with lower concrete strength, thus the interaction between the concrete core and the steel tube becomes stronger. For STCC columns, at the ultimate state, the concrete core is subjected to triaxial stress, while the steel tube is under biaxial stress. In real tests, it is complicated to measure all stresses in the concrete core and in the steel tubes. Accordingly, the confining stress induced by the steel tubes and imposed on the concrete core is hardly calculated. Therefore, many studies have attempted to use Finite Element Models (FEMs) to simulate the mechanism in STCC columns. Based on the FEM results, all stresses on STCC columns can be quantified. Authors in [12] presented an FEM in ATENA-3D software to investigate the effect of concrete strength on the compressive behavior of STCC columns. Authors in [9] developed an FEM using ABAQUS software to analyze the mechanisms of STCC short columns under axial compression, however they only focused on NSC. Authors in [13] introduced an analysis of circular STCC stub columns with some modifications to the Drucker – Prager

model in ABAQUS, and they quantified the lateral confining pressure and the interface shear stress between the concrete core and the steel tube. Authors in [15] investigated the effect of friction on axially loaded STCC short columns by utilizing an FEM. Equations considering the friction coefficient were developed to predict the load bearing capacity of STCC short columns.

From the literature review, it is apparent that numerical studies on the mechanical performance of STCC columns remain very limited with only a handful of studies considering the STCC columns with the use of NSC or HSC. Therefore additional research should be further carried out to better understand the compressive behavior of STCC columns when UHSC is infilled. Furthermore, the majority of the existing studies were concerned with the comparison of load versus displacement or load versus strain curves of STCC columns between the FEMs and the test results and very few studies dealt with the stress distribution in the steel tubes and the concrete core of STCC columns. The interaction between the concrete core and the steel tubes through the confining stress is complex and can't be measured experimentally. To address the aforementioned research gap, this paper aims to develop an FEM in ABAQUS software to simulate the mechanism of circular STCC stub columns with a wide range of concrete strengths, i.e. NSC, HSC, and UHSC. The constitutives of confined concrete were proposed based on some previous studies and some modifications to Concrete Damaged Plasticity Model (CDPM). The established FEM was verified against the collected test results. Subsequently, the confining stress and the distribution of axial load in the concrete core and the steel tube were clarified. Finally, the biaxial stress state of the steel tube was quantified by plotting the longitudinal and hoop stresses along the height of the columns.

II. FINITE ELEMENT MODEL DESCRIPTION

A. General Description

The circular STCC short columns were simulated using FEM in ABAQUS (version 6.11) [28]. Due to the symmetrical nature of the circular column, only one-eighth of the column was modelled. CAX4R elements with reduced integration and 4-node axisymmetric elements were used to model the steel tubes and the concrete core. Based on the mesh convergence studies, the element size was chosen as $t/5$, where t is the thickness of the steel tube. For short columns with the ratio of L/D (length to outer diameter) smaller than 4, the initial imperfections can be ignored in FEM. Surface-to-surface contact was employed to model the interaction between the steel tubes and concrete core. A contact surface pair including the inner surface of the steel tubes and the outer surface of the concrete core was defined. The concrete surfaces were chosen as master surfaces, while the steel surfaces were treated as master. As suggested in [18], the friction coefficient between the steel tube and concrete was taken as 0.6. Two Reference Points (RPs) were created at the center of each upper and lower cross-section. Boundary Conditions (BCs) were assigned to both reference points, while the load was applied downward at the upper reference point. The "rigid body" constraints were employed to tie the reference points to both the end surfaces of the concrete core. To ensure the load was applied only on the

concrete core, only the end surfaces of the concrete core were fixed against all degrees of freedom except for the displacement at the upper loaded end. Figure 1 shows the FEM including mesh type, boundary conditions, and loading application.
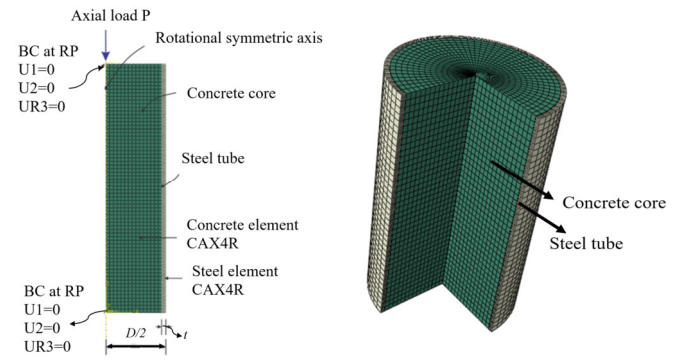

Fig. 1.   Typical FEM of a circular STCC stub column.

B. Material Models

The stress – strain relationship (σ - ε) proposed in [22] was adopted for the material model of the steel tube. This model covers a wide range of steel yield strength (f_y) from 200 to 800MPa. CDPM provided in ABAQUS was employed to simulate the compressive behavior of confined concrete. The key parameters in CDPM include the uniaxial compressive stress – strain relationship, compressive damage variable d_c ratio of the second stress invariant on the tensile meridian to that on the compressive meridian K_c, ratio of initial equibiaxial compressive yield stress to initial uniaxial compressive yield stress σ_{bo}/σ_{co}, dilation angle ψ, fracture energy G_f, viscosity, and eccentricity α. The values of K_c, ψ, and σ_{bo}/σ_{co} were calculated by using the equations suggested by [20-22], while the remaining parameters such as α, d_c, G_f, and viscosity were defined as the default values in Abaqus. The stress – strain relationship for NSC, HSC, and UHSC after taking into account the confinement effect was developed for circular STCC short columns, as can be seen in [22]. The σ - ε curve includes three stages:

The ascending branch (OA) is expressed by the equations proposed by [23]:

$$\frac{\sigma}{f_c'} = \frac{A \times X + B \times X^2}{1 + (A-2) \times X + (B+1) \times X^2} \quad 0 < \varepsilon \leq \varepsilon_{c0} \tag{1}$$

where:

$$A = \frac{E_c \times \varepsilon_{c0}}{f_c'}; B = \frac{(A-1)^2}{0.55} - 1; X = \frac{\varepsilon}{\varepsilon_{c0}} \tag{2}$$

The strain ε_{c0} at the peak stress of the unconfined concrete is calculated by [24]:

$$\varepsilon_{c0} = (-0.067 \times (f_c')^2 + 29.9 \times f_c' + 1053) \times 10^6 \tag{3}$$

The confined strain at the point B (ε_{cc}) is determined using the equation proposed in [25]:

$$\frac{\varepsilon_{cc}}{\varepsilon_{c0}} = 1 + 17.4 \times \left(\frac{f_B}{f_c'}\right)^{1.06} \tag{4}$$

$$f_B = \frac{0.03 \times f_y}{e^{0.02 \times \frac{D}{t}}} \qquad (5)$$

where f_B is the confining stress at the point B and determined by (5) suggested by [26].

The descending branch (BC) is expressed by an exponential function proposed by [27]:

$$\varepsilon_{c0} = \left(-0.067 \times \left(f_c'\right)^2 + 29.9 \times f_c' + 1053\right) \times 10^6 \qquad (6)$$

where α and β are factors determining the shape of the descending branch.

III. FINITE ELEMENT MODEL VERIFICATION AND MECHANISM ANALYSIS

The established FEM was used to simulate 3 circular STCC short columns, taken from previous studies, under axial compression. Specimens C2-30-3D-C and C1-100-3D-C reported in [16] and NB4.0-UHFB reported in [17] were considered. It is noted that, NSC (C30, $f_c = 32.7$MPa) and HSC (C90, $f_c = 105.5$MPa) were used for the specimens C2-30-3D-C and C1-100-3D-C, respectively, while UHSC (C150, $f_c = 174.2$MPa) was used for NB4.0-UHFB. Dimensions and material properties of the selected specimens are shown in Figure 2.
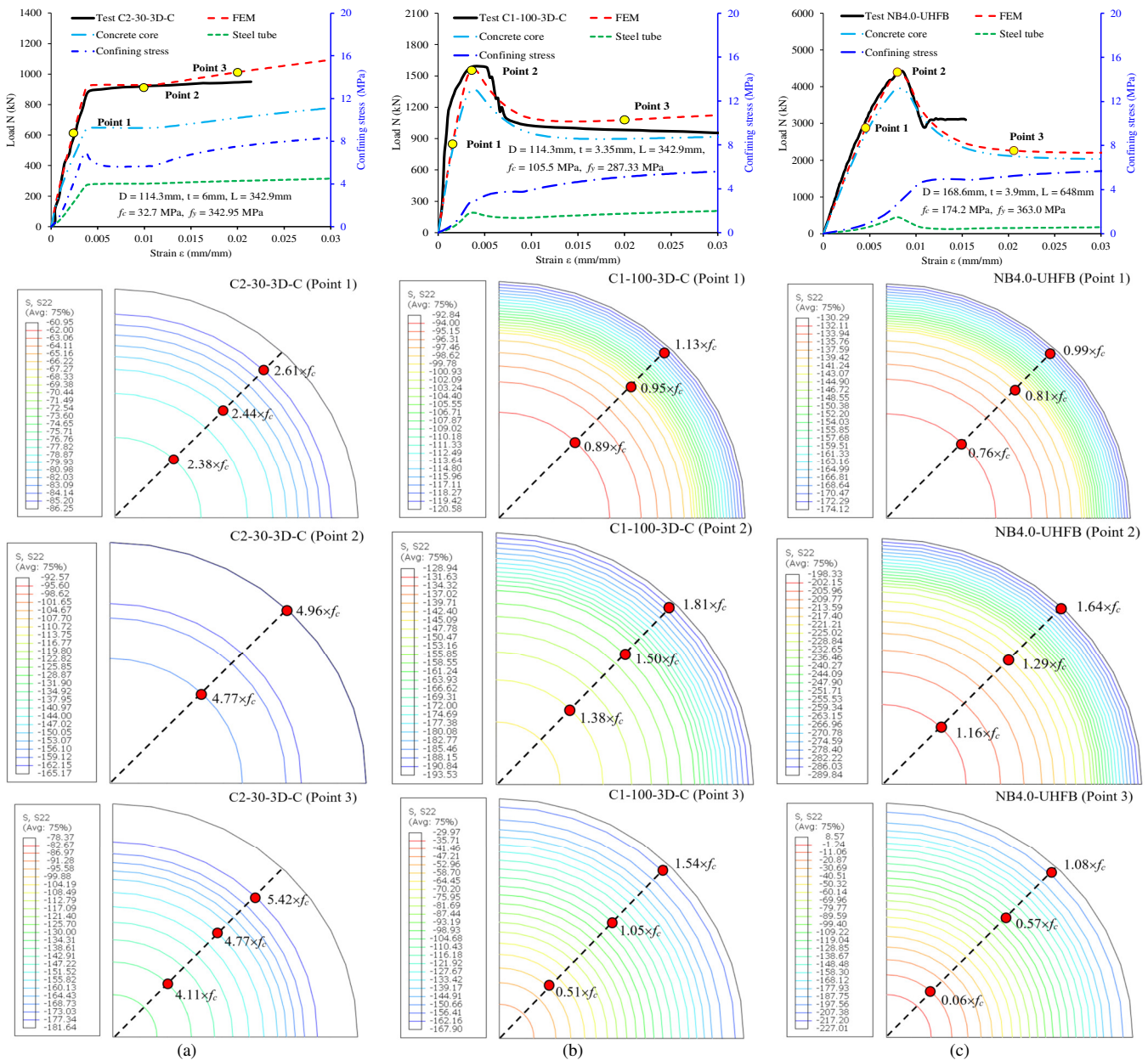

Fig. 2.   FEM verification and stress distribution on the cross section at different points. (a) Test C2-30-3D-C, (b) Test C1-100-3D-C, (c) Test NB4.0-UHFB.

In order to verify the accuracy of FEM, the load versus strain (N-ε) curves of the 3 specimens obtained from FEM were compared with those measured by the test results. It can be seen in Figure 2 that, in the ascending phase, the FEM results agree well with the measured results, but in the descending phase, there is a slight difference between the predicted and the measured curves. For the descending phase of specimens C1-100-3D-C and NB4.0-UHFB, the (N-ε) curves in FEM exhibit similar behaviors with the real tests. There is a loss of load after the peak load, followed by a horizontal branch. Overall, it can be observed that FEM predicts well the complete (N-ε) curves of all tested specimens.

Figure 2 also illustrates the distribution of the axial load between the concrete core and the steel tube and the confining stress provided by the steel tube. For NSC filled in steel tube (C2-30-3D-C), at the ultimate state, the concrete core contributed approximately 70% to the total load. However, it is observed that the concrete core carries almost the entire load for the case of HSC and UHSC. At the ultimate state, 90% of the total load was carried by the HSC core in specimen C1-100-3D-C and UHSC core in specimen NB4.0-UHFB. Furthermore, the steel tube in the case of HSC and UHSC core tends to carry less axial load before the peak stress as compared to the case of NSC. Accordingly, in the ascending branch of the (N-ε) curves, the confining stress in the case of NSC core is more intense and develops faster than in the case of HSC and UHSC. In the plastic stage, the confining stress steadily increases after reaching a stable value. Figure 2 demonstrates the distribution of longitudinal stress in the concrete section (at the top surface of the column) corresponding to three points (1, 2, and 3) in the (N-ε) curves. For the NSC core, the confining stress reaches the maximum value of 8.2MPa, which is twice the maximum value of the confining stress in the case of HSC and UHSC core. It can be seen in Figure 2 that the longitudinal stress across the concrete section is uniform along the axis of cylinder and increases gradually when the distance apart from the center of section increases. The longitudinal stress in the concrete section for the NSC core was significantly larger than that for HSC and UHSC cores. This implies that the confinement is more effective with lower concrete strength. These findings are in good agreement with the research results in [1, 8, 12-15, 22].

Figure 3 shows the distribution of longitudinal stress and hoop stress in the steel tube at the ultimate state. The ratios of stress to yield strength of steel tube (σ/f_y) were plotted along the height of the columns (h/H). It can be observed that the distribution of stresses in the steel tube is non-uniform. The longitudinal stress of the steel tube is zero and the hoop stress is relatively high at both ends of the columns. The longitudinal stress increases and the hoop stress decreases towards the column mid-height. Also, at the mid-height of the columns, the maximum value of longitudinal stress is achieved, while the hoop stress is significantly reduced. The hoop stress was maximum at $H/10$, which is quite near to the end surface of the column. The maximal values of longitudinal stress and hoop stress were about $0.55f_y$ and $0.9f_y$, $0.50f_y$, and $0.9f_y$, and $0.40f_y$ and $0.9f_y$ for NSC, HSC, and UHSC cores, respectively. The distribution of longitudinal stress in the steel tube along the column height is in line with the results reported in [9, 13, 14],

however there is a difference in the distribution of hoop stress in the steel tube between this study and the results in [9, 13, 14]. The maximum value of hoop stress in this study is generally smaller than that in [9, 13, 14]. For example, authors in [9] stated that the hoop stress is highest at the column ends. It should be noted that the confining stress depends mainly on the hoop stress. Based on the FEM results, it can be identified that confining stress is maximum at $H/10$ for circular STCC columns.
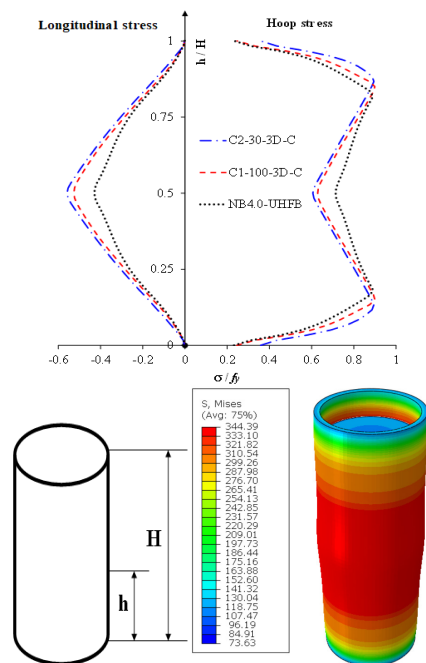

Fig. 3.   Distribution of stresses in the steel tube at the ultimate state.

IV. CONCLUSIONS

The main conclusions deriving from the FEM results of the current study are:

- The established FEM with some modifications to CDPM in ABAQUS can predict well the compressive behavior of circular STCC columns with the use of NSC, HSC, and UHSC. The distribution of stress in the concrete core and steel tube, and the confining stress can be quantified by using this FEM.

- The confining stress or confinement effect is more effective with lower concrete strength.

- The axial load carried by the concrete core becomes smaller with increasing concrete strength.

- The longitudinal stress of the steel tube is zero at both ends of the columns and increases towards the mid-height of the column, while the hoop stress is maximal at the position of $H/10$ and decreases towards the mid-height of the column.

REFERENCES

[1] M. Johansson and K. Gylltoft, "Mechanical Behavior of Circular Steel–Concrete Composite Stub Columns," *Journal of Structural Engineering*, vol. 128, no. 8, pp. 1073–1081, Aug. 2002, https://doi.org/10.1061/(ASCE)0733-9445(2002)128:8(1073).

[2] L.-H. Han, G.-H. Yao, Z.-B. Chen, and Q. Yu, "Experimental behaviours of steel tube confined concrete (STCC) columns," *Steel and Composite Structures, An International Journal*, vol. 5, no. 6, pp. 459–484, 2005, https://doi.org/10.12989/scs.2005.5.6.459.

[3] A. A. Fam, F. S. Qie, and S. Rizkalla, "Concrete-Filled Steel Tubes Subjected to Axial Compression and Lateral Cyclic Loads," *Journal of Structural Engineering*, vol. 130, no. 4, pp. 631–640, Apr. 2004, https://doi.org/10.1061/(ASCE)0733-9445(2004)130:4(631).

[4] M. D. O'Shea and R. Q. Bridge, "Design of Circular Thin-Walled Concrete Filled Steel Tubes," *Journal of Structural Engineering*, vol. 126, no. 11, pp. 1295–1303, Nov. 2000, https://doi.org/10.1061/(ASCE)0733-9445(2000)126:11(1295).

[5] M.-X. Xiong, D.-X. Xiong, and J. Y. R. Liew, "Axial performance of short concrete filled steel tubes with high- and ultra-high- strength materials," *Engineering Structures*, vol. 136, pp. 494–510, Apr. 2017, https://doi.org/10.1016/j.engstruct.2017.01.037.

[6] P. C. Nguyen, D. D. Pham, T. T. Tran, and T. Nghia-Nguyen, "Modified Numerical Modeling of Axially Loaded Concrete-Filled Steel Circular-Tube Columns," *Engineering, Technology & Applied Science Research*, vol. 11, no. 3, pp. 7094–7099, Jun. 2021, https://doi.org/10.48084/etasr.4157.

[7] A. N. Hassooni and S. R. A. Zaidee, "Behavior and Strength of Composite Columns under the Impact of Uniaxial Compression Loading," *Engineering, Technology & Applied Science Research*, vol. 12, no. 4, pp. 8843–8849, Aug. 2022, https://doi.org/10.48084/etasr.4753.

[8] Z. H. Abdulghafoor and H. A. Al-Baghdadi, "Static and Dynamic Behavior of Circularized Reinforced Concrete Columns Strengthened with Hybrid CFRP," *Engineering, Technology & Applied Science Research*, vol. 12, no. 5, pp. 9336–9341, Oct. 2022, https://doi.org/10.48084/etasr.5162.

[9] Q. Yu, Z. Tao, W. Liu, and Z.-B. Chen, "Analysis and calculations of steel tube confined concrete (STCC) stub columns," *Journal of Constructional Steel Research*, vol. 66, no. 1, pp. 53–64, Jan. 2010, https://doi.org/10.1016/j.jcsr.2009.08.003.

[10] A. L. Hoang, E. Fehling, B. Lai, D.-K. Thai, and N. V. Chau, "Experimental study on structural performance of UHPC and UHPFRC columns confined with steel tube," *Engineering Structures*, vol. 187, pp. 457–477, May 2019, https://doi.org/10.1016/j.engstruct.2019.02.063.

[11] A. Le Hoang, E. Fehling, D.-K. Thai, and C. Van Nguyen, "Evaluation of axial strength in circular STCC columns using UHPC and UHPFRC," *Journal of Constructional Steel Research*, vol. 153, pp. 533–549, Feb. 2019, https://doi.org/10.1016/j.jcsr.2018.11.001.

[12] A. Le Hoang and E. Fehling, "Numerical study of circular steel tube confined concrete (STCC) stub columns," *Journal of Constructional Steel Research*, vol. 136, pp. 238–255, Sep. 2017, https://doi.org/10.1016/j.jcsr.2017.05.020.

[13] A. Haghinejada and M. Nematzadeh, "Three-Dimensional Finite Element Analysis of Compressive Behavior of Circular Steel Tube-Confined Concrete Stub Columns by New Confinement Relationships," *Latin American Journal of Solids and Structures*, vol. 13, pp. 916–944, May 2016, https://doi.org/10.1590/1679-78252631.

[14] P. K. Gupta and H. Singh, "Numerical study of confinement in short concrete filled steel tube columns," *Latin American Journal of Solids and Structures*, vol. 11, pp. 1445–1462, Dec. 2014, https://doi.org/10.1590/S1679-78252014000800010.

[15] J. Liu, X. Zhou, and D. Gan, "Effect of friction on axially loaded stub circular tubed columns," *Advances in Structural Engineering*, vol. 19, no. 3, pp. 546–559, Mar. 2016, https://doi.org/10.1177/1369433216630125.

[16] W. L. A. de Oliveira, S. De Nardin, A. L. H. de C. El Debs, and M. K. El Debs, "Evaluation of passive confinement in CFT columns," *Journal of Constructional Steel Research*, vol. 66, no. 4, pp. 487–495, Apr. 2010, https://doi.org/10.1016/j.jcsr.2009.11.004.

[17] H. Schneider, "Zum tragverhalten kurzer, umschnürter, kreisförmiger, druckglieder aus ungefasertem UHFB," Ph.D. dissertation, University of Leipzig, Leipzig, Germany, 2006.

[18] L.-H. Han, G.-H. Yao, and Z. Tao, "Performance of concrete-filled thin-walled steel tubes under pure torsion," *Thin-Walled Structures*, vol. 45, no. 1, pp. 24–36, Jan. 2007, https://doi.org/10.1016/j.tws.2007.01.008.

[19] J. Wei, Z. Xie, W. Zhang, X. Luo, Y. Yang, and B. Chen, "Experimental study on circular steel tube-confined reinforced UHPC columns under axial loading," *Engineering Structures*, vol. 230, Mar. 2021, Art. no. 111599, https://doi.org/10.1016/j.engstruct.2020.111599.

[20] T. Yu, J. G. Teng, Y. L. Wong, and S. L. Dong, "Finite element modeling of confined concrete-I: Drucker–Prager type plasticity model," *Engineering Structures*, vol. 32, no. 3, pp. 665–679, Mar. 2010, https://doi.org/10.1016/j.engstruct.2009.11.014.

[21] V. K. Papanikolaou and A. J. Kappos, "Confinement-sensitive plasticity constitutive model for concrete in triaxial compression," *International Journal of Solids and Structures*, vol. 44, no. 21, pp. 7021–7048, Oct. 2007, https://doi.org/10.1016/j.ijsolstr.2007.03.022.

[22] Z. Tao, Z.-B. Wang, and Q. Yu, "Finite element modelling of concrete-filled steel stub columns under axial compression," *Journal of Constructional Steel Research*, vol. 89, pp. 121–131, Oct. 2013, https://doi.org/10.1016/j.jcsr.2013.07.001.

[23] A. K. Samani and M. M. Attard, "A stress–strain model for uniaxial and confined concrete under compression," *Engineering Structures*, vol. 41, pp. 335–349, Aug. 2012, https://doi.org/10.1016/j.engstruct.2012.03.027.

[24] M. A. Tasdemir, C. Tasdemir, S. Akyuz, A. D. Jefferson, F. D. Lydon, and B. I. G. Barr, "Evaluation of strains at peak stresses in concrete: A three-phase composite model approach," *Cement and Concrete Composites*, vol. 20, no. 4, pp. 301–318, Jan. 1998, https://doi.org/10.1016/S0958-9465(98)00012-2.

[25] Q. G. Xiao, J. G. Teng, and T. Yu, "Behavior and Modeling of Confined High-Strength Concrete," *Journal of Composites for Construction*, vol. 14, no. 3, pp. 249–259, Jun. 2010, https://doi.org/10.1061/(ASCE)CC.1943-5614.0000070.

[26] D.-D. Pham and P.-C. Nguyen, "Finite Element Modelling for Axially Loaded Concrete-Filled Steel Circular Tubes," in *5th International Conference on Geotechnics, Civil Engineering Works and Structures*, Singapore, Singapore, 2020, pp. 75–80, https://doi.org/10.1007/978-981-15-0802-8_8.

[27] B. Binici, "An analytical model for stress–strain behavior of confined concrete," *Engineering Structures*, vol. 27, no. 7, pp. 1040–1051, Jun. 2005, https://doi.org/10.1016/j.engstruct.2005.03.002.

[28] *Abaqus/Cae Users Manual*. USA: Hibbitt, Karlsson & Sorensen Inc, 2000.